Available online at www.sciencedirect.com
SCIENCE DIRECT
Journal of Magnetic Resonance 178 (2006) 129–135
JMR Journal of Magnetic Resonance
www.elsevier.com/locate/jmr

Hadamard NMR spectroscopy in solids

Jun Ashida [a], Ēriks Kupče [b], Jean-Paul Amoureux [c,*]

[a] Varian Technologies Japan Ltd., Tokyo, Japan
[b] Varian Ltd., Oxford, UK
[c] LCPS, CNRS-8012, USTL, Fr-59652 Villeneuve d'Ascq, France

Received 30 June 2005; revised 6 September 2005
Available online 30 September 2005

Abstract

The duration of 2D and 3D NMR experiments in solids can be reduced by several orders of magnitude by using frequency domain Hadamard encoding with long selective pulses. We demonstrate Hadamard encoded experiments in ^{13}C enriched solids samples. To avoid multiple quantum interferences, the Hadamard encoding pulses are applied sequentially rather than simultaneously in this study. Among other possible applications, dipolar assisted rotational resonance experiments and measurement of NOESY type build-up rates in proton driven spin diffusion are demonstrated.

Keywords: Solid-state NMR; Fast multi-dimensional spectra; Hadamard; Dipolar assisted rotational resonance; HETCOR; Proton driven spin diffusion

1. Introduction

Most of modern NMR experiments are based on recording of a free induction decay signal that is excited by a sequence of hard non-selective RF pulses. This is followed by Fourier transform in one or several dimensions [1]. Occasionally, selective pulses [2] are used for solvent suppression or band selective excitation. Recently, it has been demonstrated [3–6] that frequency selective Hadamard encoding in the indirectly detected dimensions, followed by Hadamard transform, can significantly reduce experiment time of 2D and 3D experiments in liquids by excluding the empty spectral regions. In this case, multiple frequency selective pulses are used for Hadamard encoding [6] that is followed by Hadamard transform and 2D or 3D spectrum reconstruction. Here, we demonstrate that the same principles are applicable to the multi-dimensional NMR spectroscopy in solids [7,8].

2. Hadamard transforms

The Hadamard transform [9] is similar to the Fourier transform in a sense that they both belong to the class of integral transforms. In general, an integral transform relating functions $g(\omega)$ and $f(t)$ via a kernel, $k(\omega,t)$, is written as:

$$g(\omega) = \int k(\omega,t) f(t) dt \tag{1}$$

In the case of Fourier transform, the kernel is a set of complex exponential functions, $\exp(i\omega t)$, while in the case of Hadamard transform the kernel is a set of Hadamard functions, that is a sub-class of the more general Walsh functions [9]. For signal processing purposes it is convenient to write Eq. (1) in the matrix form:

$$G = \mathrm{K.F} \tag{2}$$

$$G^{\mathrm{T}} = [\mathrm{G}_0, \mathrm{G}_1, \mathrm{G}_2, \mathrm{G}_3 .. \mathrm{G}_{\mathrm{N}-1}] \tag{3}$$

$$F^{\mathrm{T}} = [\mathrm{F}_0, \mathrm{F}_1, \mathrm{F}_2, \mathrm{F}_3 \ldots . \mathrm{F}_{\mathrm{N}-1}]. \tag{4}$$

Here, F and G are the input and output vector signals and the kernel K_N is a square ($N \times N$) transform matrix, which in our case is a Hadamard matrix H_N. The matrix size, N, must be a multiple of four that is larger than or equal to

* Corresponding author. Fax: +33 3 20 43 68 14.
E-mail address: jean-paul.amoureux@univ-lille1.fr (J.-P. Amoureux).

1090-7807/$ - see front matter © 2005 Elsevier Inc. All rights reserved.
doi:10.1016/j.jmr.2005.09.001

the number of resolved resonances in the Hadamard encoded dimension. The Hadamard matrices are extremely simple and consist of either +1 or −1, which for simplicity are usually replaced by + and − signs, respectively. As an example, the Hadamard matrix H_{12}, is given below:

+	−	−	−	−	−	−	−	−	−	−	−
+	+	−	+	−	−	−	+	+	+	−	+
+	+	+	−	+	−	−	−	+	+	+	−
+	−	+	+	−	+	−	−	−	+	+	+
+	+	−	+	+	−	+	−	−	−	+	+
+	+	+	−	+	+	−	+	−	−	−	+
+	+	+	+	−	+	+	−	+	−	−	−
+	−	+	+	+	−	+	+	−	+	−	−
+	−	−	+	+	+	−	+	+	−	+	−
+	−	−	−	+	+	+	−	+	+	−	+
+	+	−	−	−	+	+	+	−	+	+	−
+	−	+	−	−	−	+	+	+	−	+	+

Unlike the natural Hadamard matrices H_N, where N is a power of two, this matrix and other non-natural Hadamard matrices are asymmetric. However, it is easily verified that applying, for instance, the encoding of the first row to any of the other rows results in complete cancellation. The same is true for any other row or column. Further examples of Hadamard matrices and a more detailed description of the Hadamard transform can be found in a recent review [6].

3. Hadamard encoding

In practice, the number of resonances that need be encoded often differs from a multiple of four. For example, six resonances need be encoded in the ^{13}C-spectra of histidine and seven resonances in the case of phenyl-alanine. The problem is easily solved by choosing the nearest Hadamard matrix that can accommodate the required number of resonances (H_8 in these both cases). Note that the number of encoding pulses is still eight in these cases, while the number of encoded frequencies in each encoding pulse is less than eight. For decoding, the transpose Hadamard matrix H_N^T, which is also the inverse of H_N, is applied.

Unlike the Fourier matrix, the Hadamard matrix is real rather than complex. This considerably simplifies the Hadamard transform. More importantly, it reduces the number of Hadamard encoding steps by a factor of two. For the same reason, it improves the signal to noise ratio (S/N) of the experiment by a factor $\sqrt{2}$ as compared to that obtained with a classical Fourier transform of a similar selective frequency encoding experiment [3,6]. It must be noted that the S/N gain with respect to that observed after Fourier transform of a classical two-dimensional (2D) experiment using non-selective excitation and equally spaced t_1 increments is much larger (see below). However, it is important to remind that selective methods require the previous knowledge of the resonance frequencies, which is not the case of the classical 2D experiments.

The Hadamard transform experiments require the spin system be prepared differently from the Fourier transform experiments. Namely, the spin system must be prepared according to one of the Hadamard encoding matrices (H_N). After that, the responses of the spin system are recorded and processed by using the corresponding Hadamard decoding matrices (H_N^T). The spectra are then reconstructed as described previously [3–6].

There are two major types of Hadamard encoding that can be applied: the transverse and the longitudinal [10]. The first type of encoding scheme employs simultaneous selective excitation (Fig. 1A) or selective refocusing (Fig. 1B) pulses that are combined as described in [11]. The transverse encoding leaves the spin magnetization in the XY-plane with phase that is alternating according to the corresponding Hadamard matrices, typically between 0° and 180° (or 90° and 270°). The major disadvantages of the transverse encoding schemes are strong homogeneous losses and multiple quantum (MQ) interference effects occurring during the long selective pulses in coupled spin systems [12,13].

These interferences are considerably reduced in longitudinal encoding experiments that employ simultaneous inversion pulses (Fig. 1C). Since, in most cases the resonances in the solids spectra have no fine structure it is advantageous to employ the simplest inversion pulses, such as Gaussian [14] or e-SNOB [15] pulses. Thus, the time that spin magnetization spends in the XY plane and hence the associated interference effects are further minimized.

In systems with strong couplings such as samples rich in magnetically active isotopes, particularly in the solid state, the MQ interferences can be observed even in longitudinal encoding experiments [12,13]. Considering that T_1 relaxation in typical solids samples is relatively long, such MQ interferences can further be reduced by sequential Hadamard encoding where the corresponding sites are inverted sequentially rather than simultaneously (Fig. 1D). The bias in signal intensities resulting from relaxation during the Hadamard encoding stage can be compensated for by reversing the encoding sequence in alternate scans.

4. Results

We have first recorded a Hadamard encoded 2D proton driven spin diffusion (Figs. 2A and B) spectrum of [U–^{13}C] histidine with a mixing time of 1 ms. As expected, no cross peaks among the carbon resonances were observed in the spectrum. Histidine ^{13}C–^{13}C 2D dipolar assisted rotational resonance (DARR) [16,17] spectra with mixing time of 1ms recorded using the conventional Fourier and the Hadamard sequentially encoded pulse sequences (Figs. 2C and D) are shown in Figs. 3A and B, respectively. DARR utilizes the ^{13}C–^{1}H dipolar interaction, and is related to a combined rotor-driven and ^{1}H driven mechanism. The ^{13}C–^{1}H dipolar interaction is recovered by CW irradiation

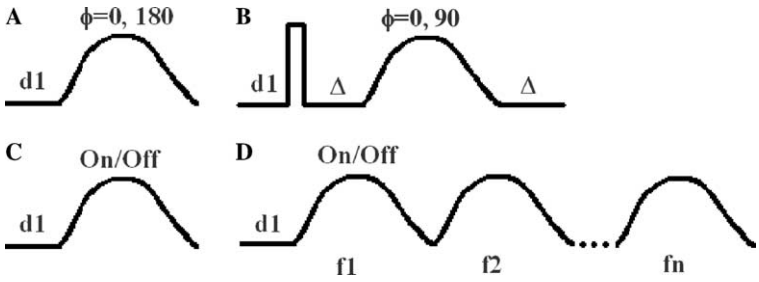

Fig. 1. Modes of Hadamard encoding. The transverse encoding uses simultaneous selective: excitation (A) or refocusing (B) schemes. The selective excitation pulses are applied with phase that is alternated between 0° and 180° according to the chosen Hadamard matrix. The selective refocusing pulses are applied with 0° or 90° phase and are preceded by a hard excitation pulse. The longitudinal encoding uses simultaneous (C) or sequential (D) selective inversion schemes. In (C) the inversion pulses are applied or omitted according to the chosen Hadamard matrix. In (D) the selective pulses are either applied or replaced by delays of equal length according to the chosen Hadamard matrix.

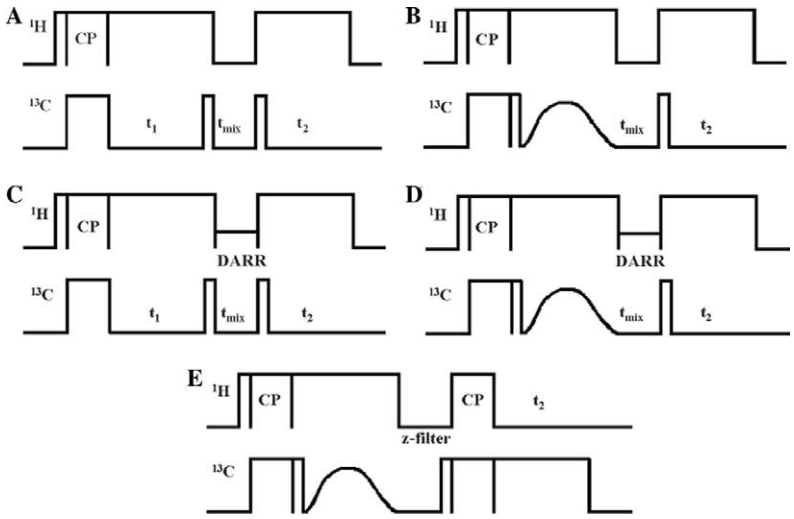

Fig. 2. Proton driven spin diffusion pulse sequence with the conventional evolution period in (A) replaced by the Hadamard encoding pulse in (B). DARR pulse sequence with either the classical evolution period (C) or the Hadamard encoding pulse (D). (E) Selective Hadamard encoded ^{1}H–^{13}C HETCOR pulse sequence using ^{1}H acquisition to be able to apply Hadamard transform in the indirect dimension. The five pulse sequences always start with a $^{1}H \rightarrow ^{13}C$ CP transfer, and use two hard $\pi/2$ pulses on the carbon channel. Decoupling is always performed during acquisition, the t_1 period and the Hadamard encoding pulses.

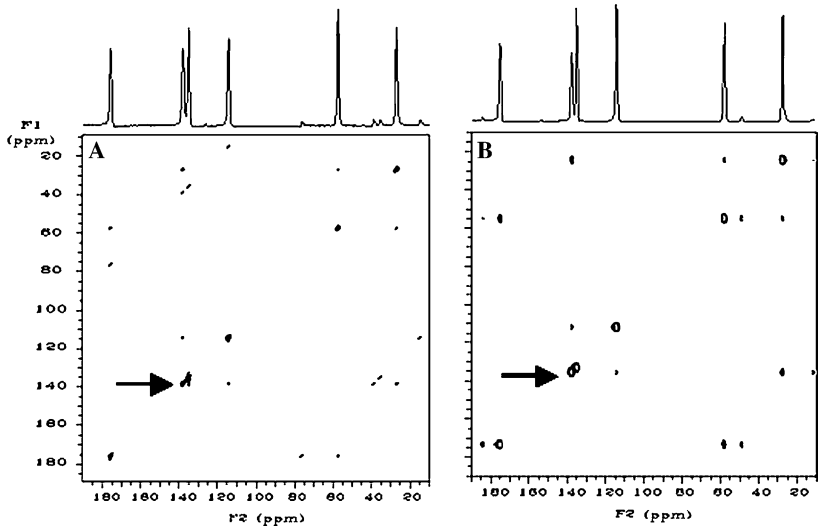

Fig. 3. [U–^{13}C] histidine 2D DARR spectra with mixing time of 1 ms recorded using the conventional Fourier (A) and the sequential Hadamard encoded (B) pulse sequence. $\nu_R = \nu_{1H} = 15$ (A) or 19 (B) kHz. Recycle delay = 10 s, eight scans. The experiment time is c.a 18 h for the conventional experiment (A) and only 10 min for the Hadamard experiment (B).

with proton field intensity satisfying the rotary-resonance condition $\nu_{1H} = n\nu_R$ ($n = 1$ or 2). The number of points in t_1 dimension for conventional phase sensitive hypercomplex 2D experiment was 400. There are six resolved peaks for histidine ^{13}C MAS spectrum, and thus we have chosen using a matrix size of eight for Hadamard encoding. Therefore, the total experiment time of Hadamard 2D DARR acquisition was only 1/100th of that of the conventional experiment. The Figs. 4A and B show traces from the conventional and the Hadamard encoded 2D DARR spectra of Fig. 3 as indicated by arrows, respectively.

We have recorded similar ^{13}C–^{13}C DARR 2D spectra on [U–^{13}C] phenyl-alanine using mixing time of 10 ms. There are eight different carbon species for phenyl-alanine, and we thus used a Hadamard matrix H_8, which required less than 3 min of experiment time. However, with magnetic field of 14.1T, the two overlapping resonances at 127 ppm, are hardly resolved and are thus treated as a single resonance with Hadamard encoding (Fig. 5).

To determine the secondary structure of molecules, it is important to obtain rough estimates of the distances between carbons from the polarization transfer rate of ^{13}C–^{13}C. This can be obtained from the build-up curves of the cross peaks determined from DARR experiments. Recording of several conventional 2D experiments with different mixing times is very time consuming. Therefore, a fast 2D method is expected to result in considerable savings of the precious spectrometer time. Fig. 6 shows the dependence of the normalized difference magnetization observed on [U–^{13}C] alanine, $\langle M_1–M_2\rangle$ (t_m)/$\langle M_1–M_2\rangle$ (0), versus the DARR mixing time at 19 kHz sample spinning speed. Total experiment time to obtain six Hadamard encoded 2D spectra of mixing times $t_{mix} = 1$, 2, 5, 10, 20, and 50 ms was only 6 min. From this dependence curve, it is obvious that C_α and C_β so that C_1 and C_α are directly bonded, in opposite to C_1 and C_β.

[U–^{13}C] alanine Hadamard encoded ^{1}H–^{13}C CP inverse-detected HETCOR [18–21] spectrum (Fig. 2E) is shown in

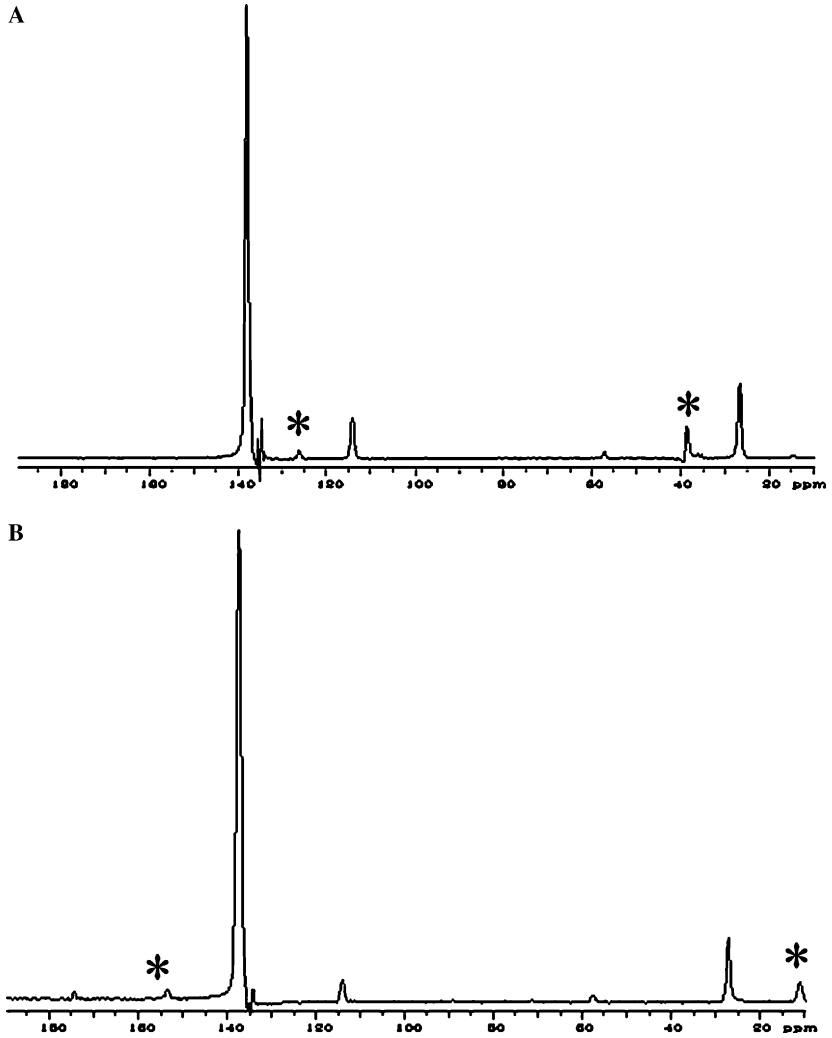

Fig. 4. F_2 traces taken from the [U–^{13}C] histidine ^{13}C–^{13}C DARR spectra shown in Fig. 3A and B as indicated by arrows at $F_1 = 139$ ppm. (A) conventional Fourier (B) sequential Hadamard encoded pulse sequence. The * indicate spinning sidebands ($\nu_R = 15$ (A) or 19 (B) kHz) of resonances situated at 27 ppm (left star) and 139 ppm (right star). The little spikes in both slices near 135 ppm arise from the tail of the diagonal resonance at 135 ppm.

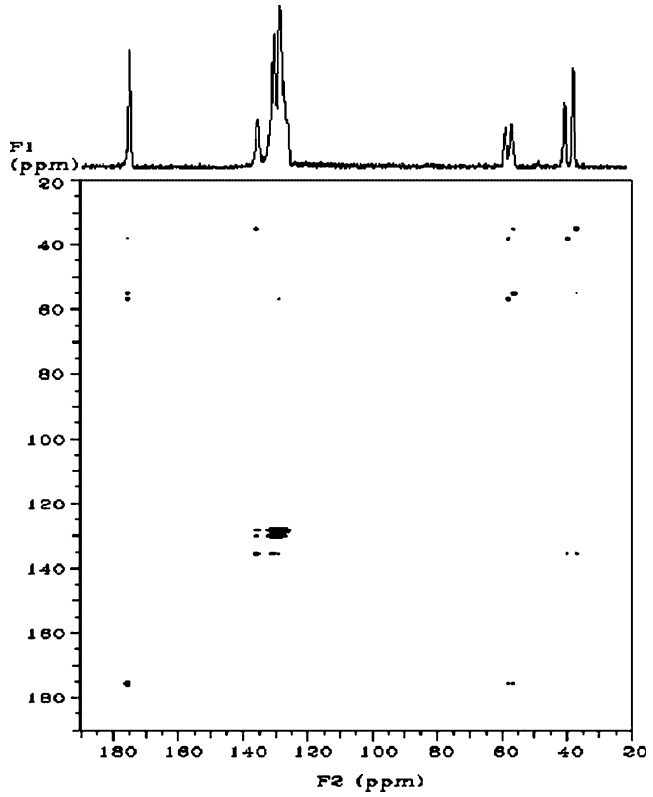

Fig. 5. DARR spectrum of [U–^{13}C] phenyl-alanine with mixing time of 10 ms. $\nu_R = \nu_{1H} = 19$ kHz. Recycle delay = 5 s, 4 scans. Hadamard matrix H_8. Total experiment time = $8 \times 4 \times 5$ s = 160 s.

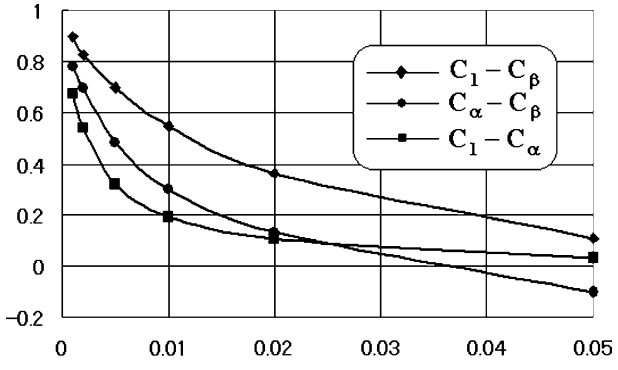

Fig. 6. Dependence of the normalized difference magnetization, $\langle M_1 - M_2\rangle(t_m)/\langle M_1 - M_2\rangle(0)$ for [U–^{13}C] alanine, versus the DARR mixing time. $\nu_R = \nu_{1H} = 19$ kHz. Recycle delay = 2 s, 8 scans. Hadamard matrix H_4. Total experiment time = $6 \times 4 \times 8 \times 2$ s = 384 s.

Fig. 7. This 2D spectrum was recorded with a Hadamard matrix H_4, with eight scans and a recycle delay of 2 s; therefore the total experiment time was only 1 min. For solid state inverse-detected HETCOR experiment involving protons, very high speed sample spinning is necessary to reduce ^{1}H–^{1}H homonuclear dipolar interactions. Therefore, the sample volume is then very limited and numerous scans are usually required to obtain conventional 2D spectrum. However, as shown in Fig. 7, a hetero-nuclear correlation spectrum could be obtained in very short time with only 20 mg sample volume by using the Hadamard encoded pulse sequence. It must be noted that the relative intensities of the ^{1}H projections (Fig. 7 right) are strongly affected by the double cross polarization process.

5. Conclusion

Experiment time of conventional nD experiments can be reduced by several orders of magnitude using Hadamard encoding and excluding the "non-useful" spectral regions. The conventional Fourier transform is replaced by Hadamard transform. Combination of selective pulses and Hadamard transform is very effective not only in separated local field 2D experiments [8], but also in correlation 2D experiments for solid state NMR. This concept is especially useful in nD experiments performed with high-field spectrometers, to resolve more easily resonances, on well crystallized samples presenting a limited number of resonances. It must be noted that the use of long selective pulses under MAS may reintroduce several interactions when the spinning speed is smaller than the size of these interactions [22]. This reintroduction may be avoided by using a multi-frequency DANTE irradiation [23] instead of long selective pulses as used in our experiments. While in the present work the method has been applied to samples with relatively sharp lines, there is no reason to believe that this is a limitation of the method. Indeed, the duration of the Hadamard encoding pulses is adjusted to the line-width and in the case of broad lines the encoding period is reduced accordingly. Hence, if there are empty spectral regions in spectra with broad resonances, the Hadamard method is still applicable.

As pointed out previously [24,25], any of the fast NMR methods is only advantageous when the S/N ratio is sufficiently high. When extensive signal averaging is required, the speed advantage is lost. However, the spectrum editing feature that is automatically included with the Hadamard method may still be useful. In this sense it differs from the other fast methods, such as the single-scan spectroscopy [26–28], the SOFAST method [29], radial sampling [30–33], and non-linear [34–36] sampling techniques. Furthermore, when it comes to comparing the sensitivity, the Hadamard method is known to outperform the Fourier method and in some cases we have indeed observed significant improvements in the signal to noise ratios per unit time in the Hadamard spectra as compared to the conventional Fourier 2D and 3D experiments (see for example Fig. 4). Further increase in sensitivity can be gained by combining the Hadamard encoding in the indirect dimensions with ANAFOR [37,38] treatment in the direct dimension.

6. Experimental

All solid state NMR spectra were performed with Varian UNITY *INOVA*-600NB with 3.2 mm T3 HXY MAS probes. All other experimental specifications are given in the figure captions.

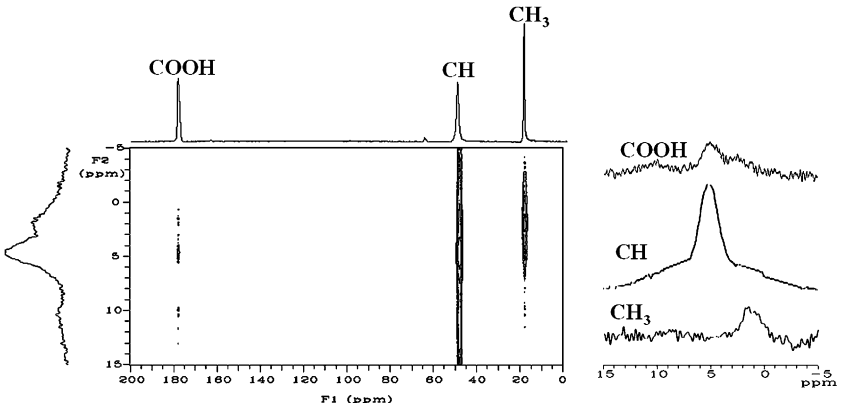

Fig. 7. [U–^{13}C] alanine Hadamard encoded ^{1}H–^{13}C HETCOR spectrum recorded with H_4 Hadamard matrix, with eight scans and a recycle delay of 2 s. $\nu_R = 17$ kHz. Total experiment time $= 4 \times 8 \times 2$ s $= 64$ s. The 1D spectra displayed on the top (^{13}C) and left side (^{1}H) are not projections nor summation of this 2D HETCOR spectrum. They are individually obtained ^{13}C CPMAS and ^{1}H MAS spectra, respectively.

Acknowledgments

J.-P.A. thank Region Nord/Pas de Calais, Europe (FEDER), CNRS, French Minister of Science, USTL, and ENSCL for funding.

References

[1] R. Ernst, G. Bodenhausen, A. Wokaun, Principles of Nuclear Magnetic Resonance in One and Two Dimensions, Clarendon Press, Oxford, 1997.
[2] R. Freeman, Spin Choreography, Spektrum, Oxford, 1997.
[3] Ē. Kupče, R. Freeman, Two-dimensional Hadamard spectroscopy, J. Magn. Reson. 162 (2003) 300–310.
[4] Ē. Kupče, R. Freeman, Fast multi-dimensional Hadamard spectroscopy, J. Magn. Reson. 163 (2003) 56–63.
[5] Ē. Kupče, R. Freeman, Fast multi-dimensional NMR of proteins, J. Biomol. NMR 25 (2003) 349–354.
[6] Ē. Kupče, T. Nishida, R. Freeman, Hadamard NMR spectroscopy, Prog. NMR. Spectrosc. 42 (2003) 95–122.
[7] This work has first been presented at AMPERE/EENC congress, Lille-France, September (2004) 6–11.
[8] J. Ashida, T. Nakai, T. Terao, Chem. Phys. Lett. 168 (1990) 523–528.
[9] K.G. Beauchamp, Transforms for Engineers. A Guide to Signal Processing, Clarendon Press, Oxford, 1987.
[10] R.A. de Graaf, In vivo NMR Spectroscop y, John Wiley and Sons, Chichester, 1998, 326–330.
[11] Ē. Kupče, R. Freeman, Template excitation in high-resolution NMR, J. Magn. Reson., Ser. A 106 (1994) 135–139.
[12] B. Ewing, S.J. Glaser, G.P. Drobny, Development and optimization of shaped pulses for the study of coupled spin systems, Chem. Phys. 147 (1990) 121–129.
[13] L. Emsley, I. Burghardt, G. Bodenhausen, J. Magn. Reson. 90 (1990) 214.
[14] C. Bauer, R. Freeman, T. Frenkiel, J. Keeler, A.J. Shaka, J. Magn. Reson. 58 (1984) 442.
[15] Ē. Kupče, J. Boyd, I.D. Campbell, Short selective pulses for biochemical applications, J. Magn. Reson., Ser B 106 (1995) 300–303.
[16] K. Takegoshi, S. Nakamura, T. Terao, ^{13}C–^{1}H dipolar-assisted rotational resonance in magic-angle spinning NMR, Chem. Phys. Lett. 344 (2001) 631–637.
[17] K. Takegoshi, S. Nakamura, T. Terao, ^{13}C–^{1}H dipolar-driven ^{13}C–^{13}C recoupling without ^{13}C rf irradiation in nuclear magnetic resonance of rotating solids, J. Chem. Phys. 118 (2003) 2325–2341.
[18] Y. Ishii, R. Tycko, Sensitivity enhancement in solid-state ^{15}N NMR by indirect detection with high-speed MAS, J. Magn. Reson. 142 (2000) 199–204.
[19] Y. Ishii, J.P. Yesinowski, R. Tycko, Sensitivity enhancement in solid-state synthetic polymers and biopolymers by detection with high-speed MAS, J. Am. Chem. Soc. 123 (2001) 2921–2922.
[20] M. Hong, S. Yamaguchi, Sensitivity-enhanced static ^{15}N NMR of solids by ^{1}H indirect detection, J. Magn. Reson. 150 (2001) 43–48.
[21] B. Reif, R.G. Griffin, ^{1}H detected ^{1}H, ^{15}N correlation spectroscopy in rotating solids, J. Magn. Reson. 160 (2003) 78–83.
[22] J. Trebosc, J.P. Amoureux, L. Delevoye, J.W. Wiench, M. Pruski, Frequency-selective measurement of heteronuclear scalar couplings in solid-state NMR, Solid State Sci. 6 (2004) 1089–1095.
[23] G.A. Morris, R. Freeman, Selective excitation in Fourier transform nuclear magnetic resonance, J. Magn. Reson. 29 (1978) 433–462.
[24] R. Freeman, Ē. Kupče, New methods for fast multi-dimensional NMR, J. Biomol. NMR 27 (2003) 101–113.
[25] R. Freeman, Ē. Kupče, Distant echoes of the accordion: reduced dimensionality, GFT-NMR and projection–reconstruction of multi-dimensional spectra, Concepts in Magn. Reson., Part A 23 (2004) 63–75.
[26] L. Frydman, T. Scherf, A. Lupulescu, The acquisition of multi-dimensional NMR spectra within a single scan, Proc. Natl. Acad. Sci. USA 99 (2002) 15859–15862.
[27] L. Frydman, A. Lupulescu, T. Sherf, Principles and features of single-scan two-dimensional NMR spectroscopy, J. Am. Chem. Soc. 125 (2003) 9204–9217.
[28] B. Shapira, A. Karton, D. Aronzon, L. Frydman, Real-time 2D NMR identification of analytes undergoing continuous chromatographic separation, J. Am. Chem. Soc. 126 (2004) 1262–1265.
[29] P. Schanda, B. Brutscher, J. Am. Chem. Soc. 127 (2005) 8014–8015.
[30] B. Bersch, E. Rossy, J. Coves, B. Brutscher, Optimized set of two-dimensional experiments for fast sequential assignment, secondary structure determination, and backbone fold validation of ^{13}C/^{15}N-labelled proteins, J. Biomol. NMR 27 (2003) 57–67.
[31] Ē. Kupče, R. Freeman, Projection-reconstruction technique for speeding up multi-dimensional NMR spectroscopy, J. Am. Chem. Soc. 126 (2004) 6429–6440.
[32] K. Ding, A. Gronenborn, Novel 2D triple-resonance NMR experiments for sequential resonance assignments of proteins, J. Magn. Reson. 156 (2002) 262–268.
[33] S. Kim, T. Szyperski, GFT NMR experiments for polypeptide backbone and ^{13}C chemical shift assignment, J. Biomol. NMR 28 (2004) 117–130.
[34] D. Rovnyak, J.C. Hoch, A.S. Stern, G. Wagner, Resolution and sensitivity of high field NMR spectroscopy, J. Biomol. NMR 30 (2004) 1–10.

[35] V. Yu Orekhov, I.V. Ibraghimov, M. Billeter, Optimizing resolution in multi-dimensional NMR by three-way decomposition, J. Biomol. NMR 27 (2003) 165–173.
[36] D. Marion, Fast acquisition of NMR spectra using Fourier transform of non-equispaced data, J. Biomol. NMR 32 (2005) 141–150.
[37] P.R. Bodart, J.P. Amoureux, F. Taulelle, ANAFOR : application of a restricted linear least squares procedure to NMR data processing, Solid State NMR 21 (2002) 1–20.
[38] G. Lippens, P.R. Bodart, F. Taulelle, J.P. Amoureux, Restricted linear least square treatment processing of heteronuclear spectra of biomolecules using the ANAFOR strategy, J. Magn. Reson. 161 (2003) 174–182.